International Journal of Pharmaceutics 422 (2012) 428–435

Contents lists available at SciVerse ScienceDirect

International Journal of Pharmaceutics

journal homepage: www.elsevier.com/locate/ijpharm

Pharmaceutical nanotechnology

Reverse aqueous microemulsions in hydrofluoroalkane propellants and their aerosol characteristics

Parthiban Selvam[a,1], Balaji Bharatwaj[a], Lionel Porcar[b,2], Sandro R.P. da Rocha[a,*]

[a] Department of Chemical Engineering and Materials Science, Wayne State University, 5050 Anthony Wayne Dr., Detroit, MI 48202, United States
[b] Institut Laue-Langevin, 6 rue Jules Horowitz, B.P. 156, F-38042 Grenoble, Cedex 9, France

ARTICLE INFO

Article history:
Received 22 July 2011
Received in revised form 6 October 2011
Accepted 18 October 2011
Available online 21 October 2011

Keywords:
Microemulsions
Metered dose inhalers
Interfacial tension
SANS
Anderson cascade impactor
Cell toxicity

ABSTRACT

In this work we describe the structure and environment of reverse aqueous microemulsions formed in 1,1,1,2-tetrafluoroethane (HFA134a) propellant in the presence of a non-ionic ethoxylated copolymer, and the aerosol characteristics of the corresponding pressurized metered dose inhaler (pMDI) formulations. The activity of selected polypropylene oxide–polyethylene oxide–polypropylene oxide ($PO_mEO_nPO_m$) amphiphiles at the HFA134a–water interface was studied using *in situ* high-pressure tensiometry, and those results were used as a guide in the selection of the most appropriate candidate surfactant for the formation of microemulsions in the compressed HFA134a. The environment and structure of the aggregates formed with the selected surfactant candidate, $PO_{22}EO_{14}PO_{22}$, was probed via UV–vis spectroscopy (molecular probe), and small angle neutron scattering (SANS), respectively. High water loading capacity in the core of the nanoaggregates was achieved in the presence of ethanol. At a water-to-surfactant molar ratio of 21 and 10% ethanol, cylindrical aggregates with a radius of 18 Å, and length of 254 Å were confirmed with SANS. Anderson Cascade Impactor (ACI) results reveal that the concentration of the excipients (C_{exp}, including surfactant, water and ethanol) has a strong effect on the aerosol characteristics of the formulations, including the respirable fraction, and the mass mean aerodynamic diameter (MMAD), and that the trend in MMAD can be predicted as a function of the C_{exp} following similar correlations to those proposed to common non-volatile excipients, indicating that the nanodroplets of water dispersed in the propellant behave similarly to molecularly solubilized compounds. Cytotoxicity studies of $PO_{22}EO_{14}PO_{22}$ were performed in A549 cells, an alveolar type II epithelial cell line, and indicate that, within the concentration range of interest, the surfactant in question decreases cell viability only lightly. The relevance of this work stems from the fact that aqueous-based HFA-pMDIs are expected to be versatile formulations, with the ability to carry a range of medically relevant hydrophilic compounds within the nanocontainers, including high potency drugs, drug combinations and biomacromolecules.

1. Introduction

Aqueous reverse microemulsions in propellant-based inhalers have been suggested as a possible vehicle for the delivery of polar drugs, including biomolecules, to and through the lungs (Patton and Byron, 2007; Rogueda, 2005; Courrier et al., 2002; Williams and Liu, 1999; Blondino, 1995; Selvam et al., 2008; Bharatwaj et al., 2010; Wu et al., 2008). Encapsulation and delivery of polar drugs in reverse aqueous microemulsions seems to be not only viable, but also very attractive, given the advantages of portable inhalers such as pMDIs (Selvam et al., 2008; Meakin et al., 2006; Steytler et al., 2003; Patel et al., 2003a,b; Peguin et al., 2006; Chokshi et al., 2009) The strategy is very simple, and consists in solubilizing the therapeutic of interest within the core of the nano-sized aqueous reverse aggregates stabilized by surfactant molecules, which are homogeneously dispersed in the propellant (Selvam et al., 2008; Wu et al., 2008; Meakin et al., 2006; Chokshi et al., 2009; Butz et al., 2002). This approach may also have some potential advantages over traditional dispersion-based (micronized drugs) pMDI formulations. For example in the case of high potency therapeutics, where drug losses due to interactions between the crystals and the canister walls may compromise the reliability of the dosage, as the total drug surface area may approach that of the walls of the container (Traini et al., 2005, 2006). This problem is expected to be mitigated by formulating the drug within the microemulsion core. Microemulsions could also be amenable to the formulation of combination therapies.

However, very few studies have reported the formulation of reverse microemulsions in propellants in general (Sommerville and

* Corresponding author. Tel.: +1 313 577 4669; fax: +1 313 578 5820.
E-mail address: sdr@eng.wayne.edu (S.R.P. da Rocha).
[1] Currently at Savara Pharma, Lawrence, KS.
[2] Current address.

0378-5173/$ – see front matter © 2011 Elsevier B.V. All rights reserved.
doi:10.1016/j.ijpharm.2011.10.038

Hickey, 2003; Sommerville et al., 2000; Courrier et al., 2004), and even fewer studies have addressed microemulsions in hydrofluoroalkanes (HFAs) (Selvam et al., 2008; Meakin et al., 2006; Steytler et al., 2003; Patel et al., 2003a,b; Chokshi et al., 2009), which are the only propellants accepted by the FDA for use in pMDIs. Within those studies that discuss microemulsions in HFA-based pMDIs, most are related to fluorinated surfactants (Steytler et al., 2003; Patel et al., 2003a,b), which are less appealing to pulmonary drug delivery applications (Lawrence and Rees, 2000). It is also worth mentioning that no study has previously addressed the aerosol characteristics of HFA-based microemulsion formulations in pMDIs. Some factors that contribute to the scarcity of studies in this area include the fact that the experiments need to be performed under pressure (Rogueda, 2005; Blondino, 1995; Peguin et al., 2006; Vervaet and Byron, 1999; Farr et al., 1987; Ridder et al., 2005; Selvam et al., 2006). The need for highly interfacially active species to facilitate the formation of such aggregates (Rogueda, 2005; Peguin et al., 2006; Vervaet and Byron, 1999; Ridder et al., 2005; Blondino and Byron, 1998; Wu et al., 2007a,b; Peguin and da Rocha, 2008; Peguin et al., 2009) has also created difficulties in the development of microemulsion-based pMDIs. In that aspect, the challenges in developing reverse-aggregate-based formulations are similar to those that exist in the design of particle-based dispersions in HFAs, where excipients containing well-solvated stabilizing moieties are required. However, solvation in HFAs, and the concept of HFA-philicity is just beginning to be understood (Rogueda, 2005; Williams and Liu, 1999; Lawrence and Rees, 2000; Vervaet and Byron, 1999; Ridder et al., 2005; Selvam et al., 2006; Peguin and da Rocha, 2008).

Based on this rationale, we report here the ability of an ethoxylated non-ionic amphiphile to form aqueous reverse aggregates in HFA134a in the presence of a water-soluble model solute, methyl orange (MO), and the effect of the reverse aggregates and other excipients on the aerosol characteristics of the corresponding formulations. The design and characterization of the microemulsions was approached rationally, through *in situ* high-pressure tensiometry, UV–vis spectroscopy, and small angle neutron scattering (SANS) experiments. The effect of non-volatiles on the aerosol characteristics were investigated via inertial impaction (Anderson Cascade Impactor, ACI). The cytotoxicity of a selected ethoxylated surfactant capable of forming water-in-HFA (W/HFA) microemulsions was studied on the A549 (alveolar type II epithelial) cell line. This work is relevant in that it demonstrates the potential of reverse-aqueous aggregates in HFAs as pMDI formulations for the non-invasive delivery of water-soluble therapeutics to and through the lungs, with particular potential relevance to high potency therapeutics, biologicals and drug combinations.

2. Materials and methods

2.1. Materials

Pluronic R® surfactants, with the general structure $PO_mEO_nPO_m$ (EO = ethylene oxide; PO = propylene oxide; m, n = average number of repeat units) were kindly donated by BASF. The surfactants were used as received. Deionized water (NANOpureII; Barnstead), with a resistivity of 18.2 MΩ cm^{-1}, was used in all experiments. Commercial (Pharma grade) HFA134a (>99.99%) was a gift from Solvay Fluor & Derivate GmbH (Hanover, Germany). Ethanol (100%) was purchased from AAPER Alcohol and Chemical Co. Methyl orange [$(CH_3)_2NC_6H_4N{=}NC_6H_4SO_3{\cdot}Na^+$, dye content – 95%] was purchased from Sigma–Aldrich. The A549 cell line was from ATCC. RPMI 1640 supplemented with L-glutamine was purchased from Invitrogen. The RPMI 1640 medium was supplemented with 10% FBS and 100 μg ml^{-1} penicillin and streptomycin, both purchased from Sigma (St. Louis, MO). Culture flasks (75 cm^2, BD Falcon) and 96-well culture plates were purchased from VWR. MTS [3-(4,5-dimethylthiazole-2-yl)-5-(3-carboxymethoxyphenyl)-2-(4-sulfophenyl)-2H, tetrazolium, inner salt] was purchased from Promega. Pressure proof glass vials (68000318) were purchased from West Pharmaceutical Services. The metering valves (EPDM Spraymiser™, 50 μl) were a gift from 3M Inc. The actuators used in all experiment were the same ones as those for the commercial Ventolin HFA® formulation.

2.2. Surfactant activity

The interfacial tension (γ) measurements were performed in a high-pressure pendant drop tensiometer as described previously (Peguin et al., 2006). Briefly, a droplet of water (or HFA134a) was injected into a high-pressure cell, in an HFA134a (aqueous) surfactant solution. Visual ports allowed for the extraction of the droplet profile. Measurements were made at 298 K and saturation pressure of the propellant mixture. The whole droplet profile was used to determine the γ with the Laplace equation (Peguin et al., 2006). After the injection of each drop, several snapshots were taken with time, until equilibration. The reported results are averages of at least three independent measurements.

2.3. Probing the environment of the reverse aggregates

In situ UV–vis spectra of HFA134a containing one or more of the following: surfactant, water, a probe, and ethanol, were obtained as described previously (Selvam et al., 2008). A known amount of surfactant (typically greater than the critical aggregation concentration) and a known volume of an aqueous solution of the solvatochromic probe MO was added to the saturated mixture in a 15 ml high-pressure glass vial (Chemglass). HFA134a or HFA134a–ethanol mixture saturated with pure water in an 'HFA saturation cell' was then added to the high pressure glass vial. Since microemulsion formation is a thermodynamically stable process; microemulsions will (spontaneously) form pseudo-solutions that are transparent due to their small (several nanometers) size. The presence and nature/structure of the microemulsions is confirmed/analyzed using UV–vis spectroscopy. After equilibration, the contents of the cell were transferred to a home-made spectroscopic high-pressure cell fitted with two sapphire windows (1 cm path length). The spectra were obtained with a Varian UV–vis spectrophotometer (Cary 3E®). The baseline for this system was obtained from the spectrum of an aqueous-saturated HFA134a or HFA134a–ethanol solution equilibrated with MO. The corrected water-to-surfactant molar ratio (W_o) was thus directly assessed; i.e., there was no need to rely on calculated water solubility in HFA since the HFA134a or HFA134a–ethanol mixture was pre-equilibrated (saturated) with water, thus allowing for the reporting of accurate water loadings.

2.4. Microstructure of the reverse aggregates

High-pressure SANS experiments in HFA134a were performed on the NG7 30-m SANS instrument at NIST (Center for Neutron Research in Gaithersburg, MD). Neutrons of wavelength $\lambda = 6$ Å with a distribution of $\Delta\lambda/\lambda = 11\%$ were incident on samples held in a custom-built high-pressure SANS cell. Sample to detector distances between 3 and 15 m were used to give a q range of $0.0035\ \text{Å}^{-1} < q < 0.45\ \text{Å}^{-1}$, where $q = (4\pi/\lambda)\sin(\theta/2)$ is the magnitude of the scattering vector. Sample scattering intensity was corrected for background, empty cell scattering and detector sensitivity. Corrected data sets were circularly averaged, placed on an absolute scale and analyzed using Igor Pro (Kline, 2006). The scattering length densities (SLD) were obtained from the

scattering length density calculator available at NIST. The SLDs for water, HFA134a, $PO_{22}EO_{14}PO_{22}$ and HFA134a + 10% (w/w) ethyl alcohol are -5.6×10^{-7}, 3.82×10^{-7}, 2.99×10^{-7}, 1.81×10^{-6} Å^{-2}, respectively. It is worth noticing that the SLD of the water–ethanol mixture is not affected by the concentration of ethanol. The aggregate size and length reported here is that of the water–ethanol mixtures (with or without solutes), including the portion of the surfactant head-group that resides in the aqueous part of the interface.

2.5. Aerosol characteristics of the pMDI formulations

The aerosol properties of the microemulsion-containing pMDI formulations were determined with an Anderson Cascade Impactor (ACI, CroPharm, Inc.) fitted with a USP induction port, and operated at a flow rate of 28.3 l min^{-1}. An exact mass of the surfactant, ethanol and MO solution were initially fed into pressure proof glass vials, and crimp-sealed with 50 μl metering valves. Subsequently, a known amount of HFA134a was added with the help of a manual syringe pump (HiP 50-6-15) and a home-built high-pressure aerosol filler. The experiments were carried out at 298 K. Before each test, 3 shots were first fired to waste. Subsequently, 15 shots were released into the impactor, with an interval of 20 s between actuations. Three independent canisters were tested for each formulation. The average and standard deviation from those three independent runs are reported here. After each run, the impactor was disassembled and the valve stem, actuator, induction port and stages were rinsed thoroughly. UV spectroscopy with a detection wavelength of 464 nm was used to quantify the fractions in each stage, which were washed with ultra-pure water. The respirable fraction (RF) and the fine particle dose (FPD) were calculated. RF is defined as the percentage of the drug present in the respirable stages of the impactor (stages 3 to filter) over the total amount of drug actuated per puff from the actuator to filter (Smyth, 2003; Gupta et al., 2003; Buttini et al., 2008; Louey et al., 2003). FPD is defined as the mass of drug (<4.7 μm) on the respirable stages of the impactor (stage 3 to terminal filter) (Gupta et al., 2003). The mass median aerodynamic diameter, MMAD, was obtained by a linear fit of a plot of the cumulative mass plotted as a function of the logarithm of the effective cut-off diameter, and recording the diameter at the midpoint of the curve fit (Buttini et al., 2008; Louey et al., 2003).

2.6. Surfactant cytotoxicity

The cytotoxic effects of a selected amphiphile ($PO_{22}EO_{14}PO_{22}$) at various concentrations were test *in vitro* on A549 cells, a human alveolar type II cell line. The cells (passage 16–21) were plated on a 75 cm^2 culture flask in RPMI 1640 medium supplemented with 10% FBS and 100 IU ml^{-1} penicillin and streptomycin. The medium was changed once every 3 days and cells were grown to 90% confluence and then sub cultured. Subsequently, A549 cells were cultured at a density 1×10^4 cells/well into a 96-well plate in RPMI 1640 medium. The cells were incubated in 200 μl of the culture media overnight after which the medium was replaced with the surfactant laden medium. Surfactant concentrations of up to 0.1 mg ml^{-1} were investigated. The cells were then allowed to stay in the surfactant medium for 24 h, after which the medium was aspirated and washed with PBS twice. Fresh medium along with the cell proliferation reagent (MTS) was added to the wells and they were incubated for 120 min. The reduction of MTS reagent to formazan by viable cells was followed spectrophotometrically at 490 nm, and the absorbance was directly correlated to the cell survival. As a positive control, cells were incubated in surfactant-free culture media. The cell viability was calculated based on the ratio of the absorbance between the surfactant treated cells and the untreated cells.

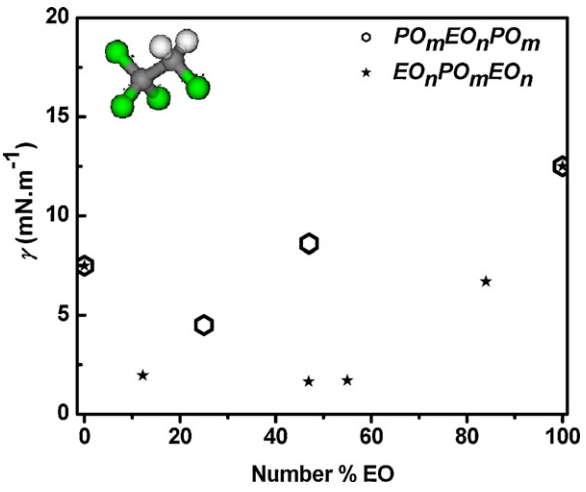

Fig. 1. Interfacial tension (□) of the HFA134a|water interface in the presence of $PO_mEO_nPO_m$ surfactants, plotted as a function of number % EO (% N_{EO}) in the surfactant molecule. Conditions were 298 K and P^{SAT} of the propellant–excipient mixture, and 1 mM surfactant concentration. The tension results for the $EO_nPO_{\sim 43}EO_n$[6] are also shown.

3. Results and discussions

3.1. Interfacial activity of $PO_mEO_nPO_m$ surfactants

The interfacial activity of the reverse Pluronic® surfactants $PO_{22}EO_{14}PO_{22}$ and $PO_{19}EO_{33}PO_{19}$ was studied at the HFA134a|W interface. Conditions were 298 K, 1 mM surfactant concentration, and saturation pressure of the propellant mixture. The results are plotted in Fig. 1 as a function of the hydrophilic-to-HFA-philic balance (HFB), in this case represented by the number % EO (% N_{EO}) in the surfactant molecule. The results for the (normal) $EO_nPO_{\sim 43}EO_n$ series and for the homopolymers EO and PO obtained in our previous work (Selvam et al., 2008) are also shown in Fig. 1.

The results indicate that $PO_{22}EO_{14}PO_{22}$, with 25% N_{EO}, is the most active at the interface, with a resulting tension of 4.5 mN m^{-1}. While not enough surfactants in the series were available to clearly scan the whole % N_{EO} range, the optimum surfactant balance (Binks, 1993) (minimum tension) seems to happen below 45% N_{EO}. For a similar surfactant class, $PO_{15}EO_nPO_{15}$, the balance point at the CO_2|Water interface was found to be between 20 and 40% N_{EO} (da Rocha et al., 1999). The solvation of compressed CO_2 and HFA134a towards PO cannot be directly compared, however, as HFA134a is known to interact very favorably with EO (the head-group) as well (Selvam et al., 2008; Peguin et al., 2006; Ridder et al., 2005; Wu et al., 2007a,b).

The effect of the surfactant architecture on its activity at the HFA134a|W interface can be assessed by comparing the results from this work for the reverse $PO_mEO_nPO_m$ series, with our previous results for the $EO_nPO_{\sim 43}EO_n$ series (Selvam et al., 2008). It can be seen that the effect of having the HFA-phile PO in the center (flanked by the head-group on both sides), is to enhance the activity of the surfactant at the HFA134a|W—note however the differences in the number of EO and PO repeat units between the two surfactant classes. Tension values as low as 1.65 mN m^{-1} were observed in our previous studies with $EO_{19}PO_{43}EO_{19}$ (Selvam et al., 2008). Similar results have been seen at the CO_2|W interface (da Rocha et al., 1999; Harrison et al., 1996; da Rocha and Johnston, 2000). One of the differences between the two classes of surfactants is the presence of two primary terminal OH groups in the regular series ($EO_nPO_{\sim 43}EO_n$) compared to two secondary OH groups in the reverse series ($PO_mEO_nPO_m$). This is expected to lead to stronger hydrogen bond donor strengths for the $EO_nPO_{\sim 43}EO_n$ surfactants

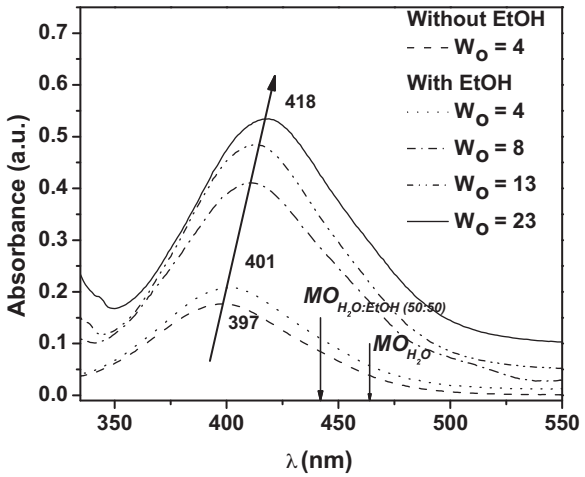

Fig. 2. Absorption spectra of HFA134a as a function of the corrected water to surfactant molar ratio (W_o). Conditions are 3 mM $PO_{22}EO_{14}PO_{22}$, at 298 K and saturation pressure of the propellant mixture. The baseline is that of HFA134a saturated with an aqueous solution of methyl orange. For system containing ethanol (EtOH), the baseline also contained EtOH at a concentration of 10% (w/w). The arrows indicates the absorption maximum for the methyl orange (MO) probe in bulk water and at 50:50 (water:EtOH). The MO peak shifts to the left for (bulk) water–EtOH mixtures with increasing concentration of EtOH.

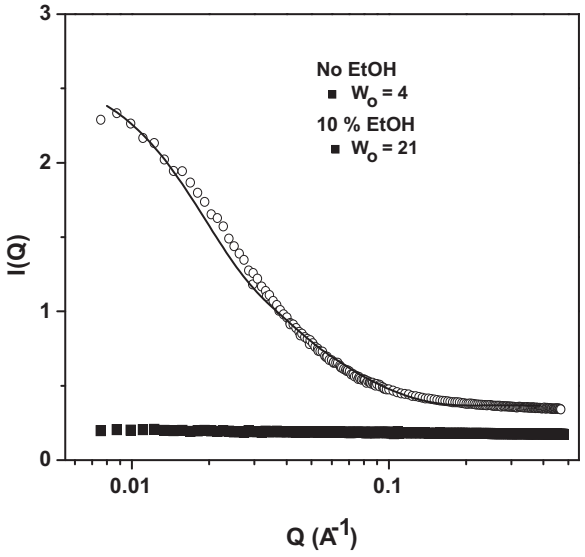

Fig. 3. Small angle neutron scattering (SANS) spectra of the reverse aqueous aggregates in HFA134a at 298 K. Surfactant ($PO_{22}EO_{14}PO_{22}$) concentration is 3 mM in the absence of EtOH, and 21.5 mM when in presence of 10% (w/w) EtOH. Corrected water-to-surfactant molar ratio (W_o) is 4 for the system without EtOH, and 21 for the run with EtOH. Lines are fits to experimental data obtained with Igor Pro.

(Takishima et al., 1997), and thus likely improved anchoring at the interface due to stronger interactions with water.

3.2. Formation of the water-in-HFA134a reverse aggregates: UV–vis spectroscopy

UV–vis spectroscopy has been previously used to probe the local environment of reverse aggregates in compressible solvents (Chokshi et al., 2009; Lay et al., 1989; Johnston et al., 1996; Liu et al., 2004). Along with a suitable solvatochromic probe, UV–vis spectroscopy is used here to indirectly investigate the nature of the aqueous phase environment of the aggregates in HFA134a. Methyl orange was selected as the solvatochromic probe as it is sensitive to the polarity of the environment it is in, and reflects changes in polarity through shifts in absorption maximum. Moreover, MO is insoluble in HFA134a (Chokshi et al., 2009). $PO_{22}EO_{14}PO_{22}$ was selected for the studies given its position (min) on the tension vs. % N_{EO} diagram—most interfacially active. The UV–vis spectra for MO in HFA134a in the presence of 3 mM $PO_{22}EO_{14}PO_{22}$ are shown in Fig. 2. The experiments were performed at 298 K and saturation pressure of the propellant mixture.

The baseline for the system in the absence of ethanol was obtained from the spectrum of water saturated HFA134a equilibrated with MO. When ethanol was present, the baseline was obtained from the spectrum of an aqueous-saturated HFA134a–ethanol solution equilibrated with MO. In the absence of EtOH, a maximum W_o of 4 is observed. At those conditions, λ_{max} is 397 nm. When contrasting the λ_{max} observed in this system to that of MO in pure (bulk) water (λ_{max} = 464 nm) (Lay et al., 1989; Johnston et al., 1996), one can conclude that, while an aqueous environment indeed exists, it is significantly different from that of bulk water, and an aqueous core is not likely being formed (Selvam et al., 2008; Chokshi et al., 2009; Ridder et al., 2005). As a comparison, for 3 mM $EO_3PO_{\sim 43}EO_3$ at similar conditions, λ_{max} increases from 399 to a maximum of 409 nm as W_o varies from 1 to 4 (Selvam et al., 2008). For aqueous aggregates of a cationic surfactant (trioctylmethylammonium chloride) in HFA134a, a small 6 nm (408–414 nm) red shift was observed as W_o varied from 0 to 12 (Li et al., 2000). These values are similar those reported for another compressible fluid (CO_2), which also suggested the presence of a unique aqueous environment. Above W_o of 4, an excess aqueous phase is observed, indicating saturation of the system in the absence of EtOH.

Higher W_o's, of up to 25, can be achieved in the presence of 3 mM $PO_{22}EO_{14}PO_{22}$ and 10% (w/w) EtOH. The UV–vis curves for W_o = 4–23 for the HFA134a–ethanol mixture are also shown in Fig. 2. An increase in λ_{max} can be observed with increasing W_o, indicating that the probe resides in a more polar environment as W_o increases. In order to understand the nature of this polar environment in the presence of EtOH, the λ_{max} for MO in bulk water–EtOH mixtures was determined. At 80/20 (w/w) (water/EtOH) λ_{max} is 462 nm. It shifts to the left (λ_{max} = 442 nm) as water concentration decreases to 50% (w/w), reaching a minimum λ_{max} of 420 nm at a water concentration of 10% (w/w). The λ_{max} in the aqueous aggregates in HFA134a at W_o = 23 is 418 nm (and shifts to the right as W_o increases), suggesting that it is closer to the expected bulk water values when compared to the system without EtOH. A λ_{max} of 420 nm was observed for 1 mM $EO_3PO_{43}EO_3$ and 10% (w/w) EtOH in HFA134a (Selvam et al., 2008; Chokshi et al., 2009), indicating that the environment of both aggregates is similar.

3.3. Microstructure of the reverse aqueous aggregates in HFA134a

While the UV–vis experiments provided an indication of the environment where the probe is located at, and thus (indirectly) of the nature of the reverse aggregates, SANS can be used to directly characterize the microstructure of the aqueous aggregates in HFA134a.

A summary of the SANS results with and without EtOH is provided in Fig. 3. The experiments were obtained at the same conditions as the UV–vis experiments discussed above; i.e., 3 mM $PO_{22}EO_{14}PO_{22}$, 298 K, saturation pressure of the propellant mixture and at a W_o = 4 (saturation for the system without EtOH), and for the system with (10%, w/w) EtOH, 21.5 mM $PO_{22}EO_{14}PO_{22}$ was added, at 298 K, saturation pressure of the propellant mixture, and W_o = 21. In the absence of ethanol and at a water loading corresponding to W_o = 4, there is no change in the scattering intensity with the scattering vector. This result is similar to that for $EO_3PO_{43}EO_3$ in HFA134a, and it indicates the presence of long hydrated polymer

Fig. 4. Physical stability of the pMDI formulation containing reverse aqueous aggregates of a saturated MO aqueous solution in HFA134a in the presence of 10% (w/w) EtOH, stabilized by 5.65% (w/w) (21.5 mM) $PO_{22}EO_{14}PO_{22}$. Conditions were 298 K, saturation pressure of the mixture and corrected water-to-surfactant molar ratio (W_o) of 21. Taken 7 months after preparation.

chains rather than reverse microemulsions (Selvam et al., 2008; Chokshi et al., 2009). This result corroborates the expectation from the UV–vis experiments.

In the presence of EtOH, however, the spectrum indicates the existence of self-assembled aggregates, which are characterized by a well-defined aqueous core. The fit to the scattering curves at W_o = 21 and 10% (w/w) EtOH, indicates that $PO_{22}EO_{14}PO_{22}$ is capable of stabilizing reverse aqueous microemulsions in HFA134a, and that the aggregates have a cylindrical geometry, with a radius of $18.1_3 \pm 0.2$ Å and a core length of $254.1_5 \pm 3.8$ Å. Reverse aqueous aggregates of $EO_3PO_{43}EO_3$ in HFA134a at W_o of 18, also have a cylindrical geometry (Selvam et al., 2008; Chokshi et al., 2009). However, $EO_3PO_{43}EO_3$, with fewer repeat units in the head-group (EO), stabilizes aggregates with a relatively smaller core radius (13.6 ± 0.5 Å), and core length (93 ± 3 Å). For water-in-xylene microemulsions stabilized by $EO_nPO_mEO_n$, it was found that the radius of the core increased (i) as the ratio of water to surfactant increased, and (ii) the number of EO in the copolymer increased (Svensson et al., 1999; Alexandridis and Anderson, 1997). Since, $PO_{22}EO_{14}PO_{22}$ has larger number of EO molecules than $EO_3PO_{43}EO_3$, the core radius is higher when stabilized with $PO_{22}EO_{14}PO_{22}$. The size of the aggregates in this study is also similar to the cylindrical micelles formed by perfluoroalkyl sulfonamide ethoxylate surfactant in aqueous system having a radius of 27 Å and a length of 290 Å (Shrestha et al., 2007).

3.4. Physical stability and aerosol characteristics of the formulations

A digital image of the reverse aqueous (saturated MO) aggregate formulation in HFA134a at 298 K is shown in Fig. 4 taken 7 months after preparation. The formulation was prepared with 10% (w/w) EtOH, 5.65% (w/w) $PO_{22}EO_{14}PO_{22}$ surfactant, and W_o = 21. The formulation was stable for long periods of time, with no excess phase observed even after the image was taken.

Table 1
Aerosol characteristics of the pMDI formulations containing saturated aqueous solutions of methyl orange (MO) within the core of the reverse aggregate in HFA134a, as a function of the % of non-volatiles.

Stages	MO (μg ± S.D.) × 10^{-2} [b]		
	5% EtOH C_{surf} = 2.90% C_{exp} = 9%	7% EtOH C_{surf} = 3.35% C_{exp} = 12%	10% EtOH C_{surf} = 5.65% C_{exp} = 18.5%
Actuator	16.5 ± 7.0	58.0 ± 7.0	268.5 ± 15.5
Induction port	108.0 ± 9.0	166.0 ± 11.0	141.5 ± 8.9
Stage 0 (<9 μm)	4.4 ± 2.1	11.0 ± 2.8	12.0 ± 5.0
Stage 1 (<5.8 μm)	4.2 ± 1.5	11.2 ± 4.1	11.0 ± 4.5
Stage 2 (<4.7 μm)	5.0 ± 1.9	8.0 ± 3.0	2.7 ± 1.3
Stage 3 (<3.3 μm)	11.0 ± 2.5	19.0 ± 4.9	9.5 ± 3.0
Stage 4 (<2.1 μm)	12.5 ± 3.0	12.0 ± 2.5	11.3 ± 5.0
Stage 5 (<1.1 μm)	6.5 ± 2.2	9.5 ± 2.2	12.0 ± 6.5
Stage 6 (<0.7 μm)	4.5 ± 1.8	4.0 ± 1.9	7.4 ± 3.0
Stage 7 (<0.4 μm)	2.5 ± 1.1	2.0 ± 0.8	4.1 ± 1.1
Filter (<0.0 μm)	<0.1	0.3 ± 0.5	<0.005
Single puff dose	175.0 ± 10.6	300.0 ± 7.9	480.0 ± 12.0
Nominal puff dose[a]	218.8 ± 8.8	343.8 ± 13.8	562.5 ± 22.5
Surface tension (mN/m)	8.81	9.10	9.53
RF (%)	21.0 ± 0.3	15.5 ± 0.2	9.2 ± 0.3
FPD (μg)	37.1 ± 2.3	46.8 ± 4.9	44.31 ± 3.3
MMAD (μm)	2.9 ± 0.2	3.4 ± 0.13	3.6 ± 0.35

[a] Nominal puff dose—calculated based on the concentration of MO in the formulation and the size of the valve reservoir. Error estimated based on the error in weighing the material.
[b] N = 3; 15 puffs each run.

Anderson Cascade Impactor (ACI) was employed to investigate the quantitative aerosol characteristics of the pMDI formulations containing MO loaded into the core of the reverse aqueous aggregates in HFA134a. The results are summarized in Table 1. They represent averages of three runs for each formulation. The ACI results as a function of the volatiles % shown in Table 1 are recast in Fig. 5 as percentages. Note that while the table contains the raw information—all properties of the aerosol can be derived from the table, a figure of percentages is the best way to directly compare the aerosol quality of the different formulations, but cannot be used to extract other relevant information regarding the characteristics of the aerosols. The formulation at the highest EtOH concentration contains 10% (w/w) EtOH, 5.65% surfactant (21.5 mM) and a W_o = 21, which is the same formulation used in the SANS study. The MO was at saturation (60 mM aqueous solution). As the EtOH concentration decreases, the water and surfactant loading also decrease. Appropriate proportions were used (for the

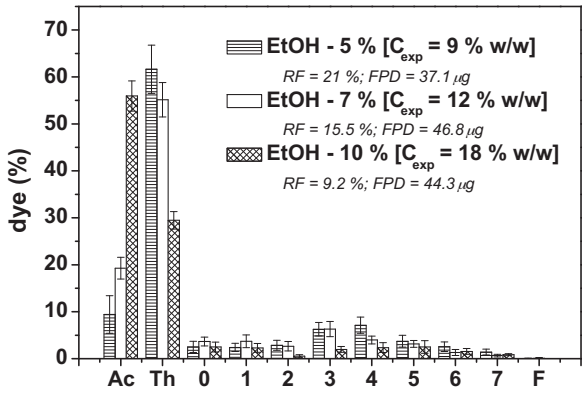

Fig. 5. Aerodynamic particle size distribution (%) of reverse aqueous (saturated MO aqueous solution) aggregates in HFA134a as determined by ACI. Studies were performed as a function of EtOH concentration (5, 7 and 10%, w/w propellant) or concentration of non-volatile excipient (%, w/w propellant of water + surfactant + EtOH, of 9, 12 and 18.5%). Conditions were 298 K saturation pressure of the mixture and corrected water-to-surfactant molar ratio (W_o) of 21.

formulation to remain as a single clear phase), and those are described in Table 1 as surfactant concentration ($C_{surfactant}$) and total excipient concentration ($C_{exp} = C_{EtOH} + C_{water} + C_{surfactant}$), where % are weight percent overall.

One can observe that the C_{exp} has a pronounced effect in the RF. The RF increases from 9.2% to 21.0% as C_{exp} decreases from 18.5 to 9.0%. This is related to the fact that while the amount of MO retained in the induction port (IP) is not greatly different in the various formulations, the concentration retained in the actuator (Ac) increases dramatically (from 10 to 55%) as C_{exp} varies from 9 to 18.5%. Previous studies on the effect of ethanol (just ethanol) concentration on HFA134a formulations indicated that the general effect of increasing ethanol concentration on the larger population of droplets (≥10 μm) during atomization (actuation) was to shift the mode to larger droplet sizes and to increase the proportion of these larger droplets.51 (Hugh et al., 2003). Droplets that constitute the larger mode in the particle size distribution (approximately 10 μm) exhibited insufficient evaporation after actuation to become "respirable." Due to this insufficient evaporation of the propellant from these large droplets, an increase in actuator deposition with increasing ethanol concentration in the pMDI formulations is observed. It is interesting to contrast our study with that for a cyclosporine solution formulation in HFA134a containing 0.1% (w/w) of cyclosporine in HFA134a or HFA134a–ethanol mixture (Myrdal et al., 2004). An increase of 4.8% in Ac deposition was found in that study as the amount of ethanol in the formulation increased from 0 to 10% (w/w). This increase in Ac deposition is much more modest than that observed in our study, suggesting that the presence of other non-volatile excipients (water and surfactant in our case) also play an important role in determining the final aerosol characteristics (Hugh et al., 2003; Smyth, 2003).

However, the FPD also increases as the C_{exp} increases, reaching a plateau at around 12–18.5%. The initial increase in FPD with C_{exp} is due to the increase in drug loading. However, at higher C_{exp}, the increase in drug loading was negated by a decrease in the respirable deposition. Similar trend has been noted in a study of beclomethasone dipropionate, a solution formulation in HFA134a–ethanol mixture. The FPD increased with increasing ethanol concentration in the formulation until a plateau was reached at an ethanol concentration of 10–15% (w/w) (Gupta et al., 2003). These effects are attributed to the fact that the vapor pressure of the HFA134a mixture decreases as the concentration of excipient increases (Hugh et al., 2003; Brambilla et al., 1999). Upon the addition of 11.85% (w/w) EtOH to HFA134a at 298 K, the saturation pressure is reduced from 0.665 MPa to 0.572 MPa (Williams and Liu, 1998). During actuation of an HFA–ethanol solution mixture from a pMDI, the amount of fine particles in the spray would be inversely proportional to the orifice diameter and proportional to the square root of the vapor pressure. Thus as vapor pressure of the mixture decreases, the fine particle diameter increases and the proportion of the delivered dose depositing in the throat also increases, resulting in lower RFs (Brambilla et al., 1999; Clark, 1991; Williams and Liu, 1998) Hence, formulations with HFA/ethanol mixtures result in lower RFs, and higher IP depositions due to decreased vapor pressures (Smyth, 2003; Hugh et al., 2003; Brambilla et al., 1999).

The macroscopic discussion above necessarily includes any potential surface energy effects. However, as far as we know, there has been no previous work on the effect of ethanol on the surface tension of HFAs. A rough estimation of the surface tension of the ethanol–HFA mixture can be obtained; however, using a simple volume fraction weighted average of the interfacial energy of the pure components. These values are listed in Table 1. Comparing the RF with the surface tension values of the HFA–ethanol mixture (we use surface tension of pure EtOH as 22.39 mN/m (Sun and Shekunov, 2003); pure HFA134a as 8.10 mN/m (Peguin et al., 2006)), we see that as the surface tension increases, the RF decreases. Previous studies indicate that as ethanol concentration in HFA134a–ethanol mixtures increases from 2.5% to 50%, the MMAD increases from 0.48 μm to 1.54 μm and the RF decreases from 49.6% to 4.7% (Smyth, 2003). Myrdal et al. noted that the influence of ethanol concentration on droplet size is much larger than would be expected based on the change in vapor pressure alone, indicating that there are formulation properties other than vapor pressure (possibly surface tension) that substantially affect the size of the droplets formed during atomization (Stein and Myrdal, 2004). Thus a reasonable estimation for the upper limit of ethanol concentration in ethanol–HFA formulations to obtain realistic RFs (>15%) is 10% (w/w).

Previous studies indicated pMDIs formulations containing HFA134a and ethanol mixtures resulted in predominantly bimodal distributions due to the formation of secondary droplets from primary droplets after actuation (Hugh et al., 2003). During actuation, primary droplets are formed from the pre-atomized HFA aerosols either by internal flash evaporation or aerodynamic breakup (Hugh et al., 2003; Finlay, 2001). Primary droplet formation can be followed by secondary breakup if the changes in relative velocity are sufficient. The addition of a vapor pressure suppressant such as ethanol is likely to reduce the initial relative velocities of primary droplets resulting in secondary droplet formation. The particle size distribution at 7% and 10% EtOH concentration is, therefore, expected to be bimodal. Moreover, as the C_{exp} increases from 9% to 18.5%, the MMAD of the reverse microemulsions formulated in this work increases from 2.9 μm to 3.6 μm. It has been argued that the MMAD of the emitted aerosol particle is directly proportional to the cube root of the concentration of non-volatiles (Brambilla et al., 1999). Based on this principle, the MMAD at 18.5% is estimated to be 3.6 μm, which is in perfect agreement with the experimental value. Hence, as the amount of non-volatiles increases, the aerodynamic particle size increases resulting in a higher portion of the delivered dose impacting in the right-angled IP of the apparatus or on the upper stages of the impactor. It is interesting to observe that the nanodroplets of water dispersed in the propellant seem to affect the overall aerosol characteristics of the formulation as molecularly solubilized non-volatile excipients.

3.5. Cytotoxity of $PO_{22}EO_{14}PO_{22}$

One further consideration regarding the formulation is the cytotoxicity of the surfactant. The MTS assay was used in order to assess the *in vitro* toxicity of $PO_{22}EO_{14}PO_{22}$ on the A549 (alveolar type II) cell line (Wu et al., 2007a,b). Based on the ACI studies discussed above, the amount of surfactant expected to reach the lower airways (stages 3 – F) for the formulation with the largest surfactant concentration is 0.345 mg per actuation (based on the RF of that formulation). Assuming the worst case scenario, where all of the surfactant ends up in the alveolar region, which has an estimated total volume of fluid of approximately 7 ml (Patton, 1996), a maximum concentration of 0.1 mg ml^{-1} of surfactant is estimated. We, therefore, investigated the cytotoxicity of the surfactant within that range. The MTS results are summarized in Fig. 6. They represent an average (and deviation) of 5 independent experiments.

At low concentrations (0.01 mg ml^{-1} to 0.02 mg ml^{-1}), the surfactant seems to exhibit no toxicity, as indicated by the high cell viability. A slight increase in the cytotoxicity of $PO_{22}EO_{14}PO_{22}$ is observed at higher concentrations (0.04 mg ml^{-1} and above), with 90% cell viability observed at 0.05 mg ml^{-1}. The surfactant toxicity increased significantly at 0.1 mg ml^{-1}, with a cell viability of 64%. Several previous works have discussed the cytotoxic effects of nonionic surfactants on lung epithelial cell lines (Alakhov et al., 1999; Tsujino et al., 1999; Warisnoicharoen et al., 2003). Surfactants like Brij® 97 and Tween® 80 were shown to have a 50% cell kill at a concentration of around 0.1 mg ml^{-1} on 16HBE14o- and A549

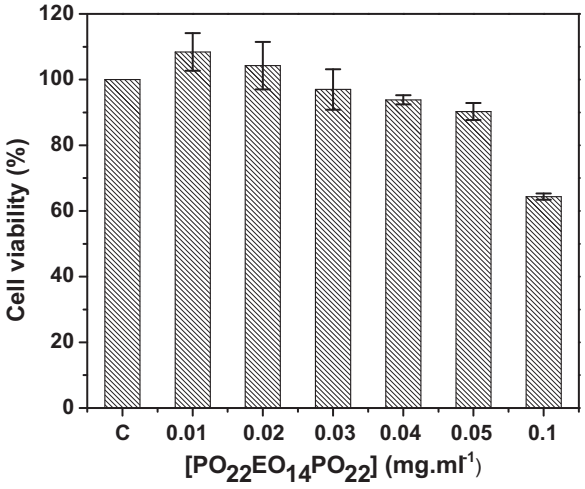

Fig. 6. Viability of the lung alveolar epithelial A549 cell line as a function of the concentration of $PO_{22}EO_{14}PO_{22}$.

cell lines respectively (Tsujino et al., 1999; Warisnoicharoen et al., 2003). Notably, Brij® 97s effect was inhibitory even at 0.01 mg ml^{-1} with a cell kill of about 20%. Pluronic® block copolymers along with antineoplastic agents have been observed to enhance the cytotoxic effect of the drug by increasing the drug permeability into the cell monolayers (Alakhov et al., 1996; Batrakova et al., 1999; Kabanov et al., 2002). For instance, 100% cell kill was achieved by the cancer drug daunorubicin at a concentration of 1% by weight of the surfactant Pluronic P85 (Kabanov et al., 2002). Based on the *in vitro* studies, two to three actuations per day of such formulation would result in no decrease in cell viability due to the presence of surfactant. Based on cell viability, methyl orange solubility studies and the aerosol dispersion studies, it is estimated that nearly 40–60 mcg of a polar therapeutic or biomacromolecule can be delivered using the proposed formulation. This demonstrates the potential of reverse-aqueous aggregates in HFAs as pMDI formulations for the non-invasive delivery of water-soluble therapeutics to and through the lungs, with particular potential relevance to high potency anticancer therapeutics and biomacromolecules (Rogueda, 2005; Courrier et al., 2002; Selvam et al., 2008; Lawrence and Rees, 2000; Patton et al., 1999).

4. Conclusions

The interfacial activity of $PO_mEO_nPO_m$ surfactants was studied at the HFA134a|W interface using *in situ* high-pressure pendant drop tensiometry. This surfactant class is capable of reducing the tension of the HFA134a|W interface to as low as 4.5 mN m^{-1}, point at which the HFB is estimated to be ~25% N_{EO}. $PO_mEO_nPO_m$ have weaker hydrogen bond donors on the terminal groups compared to the $EO_nPO_{\sim 43}EO_n$, and a confined EO in the middle position that seems to inhibit conformational changes, possibly causing a reduction in their activity at the HFA134a|W interface. The polar nature and the microstructure of the reverse aggregates were studied using *in situ* high-pressure UV–vis spectroscopy and SANS. In the absence of EtOH, presence of long hydrated polymer chains rather than reverse microemulsions is observed. However upon adding EtOH, cylindrical microemulsions with a core radius of $18.1_3 \pm 0.2$ Å and a core length of $254.1_5 \pm 3.8$ Å were detected.

The presence of EtOH and other non-volatiles (water and surfactant) reduce the vapor pressure of the aerosol mixture, thus causing an increase in the diameter of the emitted aerosol droplets. High depositions in the actuator and induction port are thus observed. However, FPFs of ca. 20% can be consistently achieved. These nanoaggregates seem to behave as molecularly solubilized excipients with regards to the aerosol properties of the pMDI formulations. Low toxicity was observed at the desired surfactant concentration range, indicating the fairly benign nature of $PO_{22}EO_{14}PO_{22}$.

The relevance from this work stems from the fact that the proposed pMDI formulations may find applications in the regional delivery of highly potency therapeutics to the lungs, as reliable delivery of small dosages may be more consistently achieved, since the drug is encapsulated within the water core, and adhesion between the walls of the container and the drug (when compared to drugs formulated as crystals) are less of a concern (Traini et al., 2006; Price et al., 2002). Reverse microemulsion-based formulations have other potential advantages over other suspension- and solution-based formulations in that they may provide an opportunity to deliver drug combinations (e.g. therapeutic biomolecules and or other small polar drug) without the need of extensive reformulation.

Acknowledgements

NSF-CBET (grant no. 0933144) for financial support; a Thomas C. Rumble Fellowship for PS; Nano@WSU RA-ship for BB; Solvay Fluor und Derivate GmbH & Co., Hannover, Germany, for the HFA134a samples; BASF for the surfactants; West Pharmaceuticals and 3M, for the glass vials and metering valves, respectively. We acknowledge the support of the National Institute of Standards and Technology, U.S. Department of Commerce, in providing the neutron-research facilities used in this work. The mention of commercial products does not imply endorsement by NIST, nor does it imply that the materials or equipment identified are necessarily the best available for the purpose.

References

Alakhov, V., Klinski, E., Li, S., Pietrzynski, G., Venne, A., Batrakova, E., Bronitch, T., Kabanov, A., 1999. Block copolymer-based formulation of doxorubicin. From cell screen to clinical trials. Colloids Surf. B 16, 113–134.

Alakhov, V., Moskaleva, E.Y., Batrakova, E.V., Kabanov, A.V., 1996. Hypersensitization of multidrug resistant human ovarian carcinoma cells by Pluronic P85 block copolymer. Bioconjug. Chem. 7, 209–216.

Alexandridis, P., Andersson, K., 1997. Reverse micelle formation and water solubilization by polyoxyalkylene block copolymers in organic solvent. J. Phys. Chem. B 101, 8103–8111.

Scattering Length Density Calculator. NIST Center for Neutron Research, Gaithersburg, MD, USA, http://www.ncnr.nist.gov/resources/sldcalc.html.

Batrakova, E., Li, S., Miller, D.W., Kabanov, A.V., 1999. Pluronic P85 increases permeability of a broad spectrum of drugs in polarized BBMEC and Caco-2 cell monolayers. Pharmaceutica 16, 1366–1372.

Bharatwaj, B., Wu, L., Whittum-Hudson, J.A., da Rocha, S.R.P., 2010. The potential for the noninvasive delivery of polymeric nanocarriers using propellant-based inhalers in the treatment of Chlamydial respiratory infections. Biomaterials 31, 7376–7385.

Binks, B.P., 1993. Relationship between microemulsion phase behavior and macroemulsion type in systems containing nonionic surfactant. Langmuir 9, 25–28.

Blondino, F.E., 1995. Novel Solution Aerosols for Inhalation. Virginia Commonwealth University.

Blondino, F., Byron, P.R., 1998. Surfactant dissolution and water solubilization in chlorine-free liquified gas propellants. Drug Dev. Ind. Pharmacy 24, 935–945.

Brambilla, G., Ganderton, D., Garzia, R., Lewis, D., Meaking, B.J., Ventura, P., 1999. Modulation of aerosol clouds produced by pressurised inhalation aerosols. Int. J. Pharm. 186, 53–61.

Buttini, F., Colombo, P., Wenger, M.P.E., Mesquida, P., Marriott, C., Jones, S.A., 2008. Back to basics: the development of a simple, homogenous, two component dry powder inhaler formulation for the delivery of budesonide using miscible vinyl polymers. J. Pharm. Sci. 97, 1257–1267.

Butz, N., Porté, C., Courrier, H., Krafft, M.P., Vandamme Th, F., 2002. Reverse water-in-fluorocarbon emulsions for use in pressurized metered-dose inhalers containing hydrofluoroalkane propellants. Int. J. Pharm. 238, 257–269.

Chokshi, U., Selvam, P., Porcar, L., da Rocha, S.R.P., 2009. Reverse aqueous emulsions and microemulsions in HFA227 propellant stabilized by non-ionic ethoxylated amphiphiles. Int. J. Pharm. 369, 176–184.

Clark, A.R., 1991. Metered Atomisation for Respiratory Drug Delivery. Loughborough Univ. of Technology, United Kingdom.

Courrier, H.M., Butz, N., Vandamme, Th. F., 2002. Pulmonary drug delivery systems: recent developments and prospects. Crit. Rev. Ther. Drug Carrier Syst. 19, 425–498.
Courrier, H.M., Vandamme, Th.F., Krafft, M.P., 2004. Reverse water-in-fluorocarbon emulsions and microemulsions obtained with a fluorinated surfactant. Colloids Surf. A 244, 141–148.
Farr, S.J., Kellaway, I.W., Meakin, B., 1987. Assessing the potential of aerosol-generated liposomes from pressurised pack formulations. J. Control. Release 5, 119–127.
Finlay, W.H., 2001. The Mechanics of Inhaled Pharmaceutical Aerosols. Academic Press, London, UK.
Gupta, A., Stein, S.W., Myrdal, P.B., 2003. Balancing ethanol cosolvent concentration with product performance in 134a-based pressurized metered dose inhalers. J. Aerosol Med. 16, 167–174.
Harrison, K.L., Johnston, K.P., Sanchez, I.C., 1996. Effect of surfactants on the interfacial tension between supercritical carbon dioxide and polyethylene glycol. Langmuir 12, 2637–2644.
Smyth, H.D.C., Hickey, A.J., 2003. Multimodal particle size distributions emitted from HFA-134a solution pressurized metered-dose inhalers. AAPS PharmSciTech 4, 76–86.
Johnston, K.P., Harrison, K.L., Clarke, M.J., Howdle, S.M., Heitz, M.P., Bright, F.V., Carlier, C., Randolph, T.W., 1996. Water-in-carbon dioxide microemulsions: an environment for hydrophiles including proteins. Science 271, 624–626.
Kabanov, A.V., Batrakova, E.V., Alakhov, V., 2002. Pluronic® block copolymers as novel polymer therapeutics for drug and gene delivery. J. Control. Release 82, 189–212.
Kline, S.R., 2006. Reduction and analysis of SANS and USANS data using IGOR Pro. J. Appl. Cryst. 39, 895–900.
Lawrence, M.J., Rees, G.D., 2000. Microemulsion-based media as novel drug delivery systems. Adv. Drug Deliv. Rev. 45, 89–121.
Lay, M.B., Drummond, C.J., Thistlethwaite, P.J., Grieser, F., 1989. ET(30) as a probe for the interfacial microenvironment of water-in-oil microemulsions. J. Colloid Interface Sci. 128, 602–604.
Li, J.-R., Lee, Y.-M., Yu, T., 2000. Solubilization of hydrophilic compounds in 1,1,1,2-tetrafluoroethane with a cationic surfactant. Anal. Chem. 72, 1348–1351.
Liu, J., Ikushima, Y., Shervani, Z., 2004. Investigation on the solubilization of organic dyes and micro-polarity in AOT water-in-CO_2 microemulsions with fluorinated co-surfactant by using UV–Vis spectroscopy. J. Supercrit. Fluid 32, 97–103.
Louey, M.D., Razia, S., Stewart, P.J., 2003. Influence of physico-chemical carrier properties on the in vitro aerosol deposition from interactive mixtures. Int. J. Pharm. 252, 87–98.
Meakin, B.J., Lewis, D. A., Berrill, S.A., Davies, R.J., 2006. Solubilisation of drugs in HFA propellant by means of emulsions, July 27. PCT/EP03/05800.
Myrdal, P.B., Karlage, K.L., Stein, S.W., Brown, B.A., Haynes, A., 2004. Optimized dose delivery of the peptide cyclosporine using hydrofluoroalkane based metered dose inhalers. J. Pharm. Sci. 93, 1054–1061.
Patel, N., Marlow, M., Lawrence, M.J., 2003a. Fluorinated ionic surfactant microemulsions in hydrofluorocarbon 134a (HFC 134a). J. Colloid Interface Sci. 258, 354–362.
Patel, N., Marlow, M., Lawrence, M.J., 2003b. Formation of fluorinated nonionic surfactant microemulsions in hydrofluorocarbon 134a (HFC 134a). J. Colloid Interface Sci. 258, 345–353.
Patton, J.S., 1996. Mechanisms of macromolecule absorption by the lungs. Adv. Drug Deliv. Rev. 19, 3–36.
Patton, J.S., Byron, P.R., 2007. Inhaling medicines: delivering drugs to the body through the lungs. Nat. Rev. Drug Discov. 6, 67–74.
Patton, J.S., Bukar, J., Nagarajan, S., 1999. Inhaled insulin. Adv. Drug Deliv. Rev. 35, 235–247.
Peguin, R.P.S., da Rocha, S.R.P., 2008. Solvent–solute interactions in hydrofluoroalkane propellants. J. Phys. Chem. B 112, 8084–8094.
Peguin, R.P.S., Kamath, G., Potoff, J.J., da Rocha, S.R.P., 2009. All-atom force field for the prediction of vapor–liquid equilibria and interfacial properties of HFA134a. J. Phys. Chem. B 113, 178–187.
Peguin, R.P.S., Selvam, P., da Rocha, S.R.P., 2006. Microscopic and thermodynamic properties of the HFA134a-water interface: atomistic computer simulations and tensiometry under pressure. Langmuir 22, 8826–8830.
Price, R., Young, P.M., Edge, S., Staniforth, J.N., 2002. The influence of relative humidity on particulate interactions in carrier-based dry powder inhaler formulations. Int. J. Pharm. 246, 47–59.
Ridder, K.B., Davies-Cutting, C.J., Kellaway, I.W., 2005. Surfactant solubility and aggregate orientation in hydrofluoroalkanes. Int. J. Pharm. 295, 57–65.
da Rocha, S.R.P., Johnston, K.P., 2000. Interfacial thermodynamics of surfactants at the CO_2–water interface. Langmuir 16, 3690–3695.
da Rocha, S.R.P., Harrison, K.L., Johnston, K.P., 1999. Effect of surfactants on the interfacial tension and emulsion formation between water and carbon dioxide. Langmuir 15, 419–428.
Rogueda, P.G., 2005. Novel hydrofluoroalkane suspension formulations for respiratory drug delivery. Expert Opin. Drug Deliv. 2, 625–638.
Selvam, P., Chokshi, U., Gouch, A., Wu, L., Porcar, L., da Rocha, S.R.P., 2008. Ethoxylated copolymer surfactants for the HFA134a–water interface: interfacial activity, aggregate microstructure and biomolecule uptake. Soft Matter 4, 357.
Selvam, P., Peguin, R.P.S., Chokshi, U., da Rocha, S.R.P., 2006. Surfactant Design for the 1,1,1,2-tetrafluoroethane–water interface: ab initio calculations and in situ high-pressure tensiometry. Langmuir 22, 8675–8683.
Shrestha, L.K., Sharma, S.C., Sato, T., Glatter, O., Aramaki, K., 2007. Small-angle X-ray scattering (SAXS) study on nonionic fluorinated micelles in aqueous system. J. Colloid Interface Sci. 316, 815–824.
Smyth, H.D.C., 2003. The influence of formulation variables on the performance of alternative propellant-driven metered dose inhalers. Adv. Drug Deliv. Rev. 55, 807–828.
Sommerville, M.L., Cain, J.B., Johnson Jr., C.S., Hickey, A.J., Hickey, 2000. Lecithin inverse microemulsions for the pulmonary delivery of polar compounds utilizing dimethylether and propane as propellants. Pharm. Dev. Technol. 5, 219–230.
Sommerville, M.L., Hickey, A.J., 2003. Aerosol generation by metered-dose inhalers containing dimethyl ether/propane inverse microemulsions. AAPS PharmSciTech 4, 455–461.
Stein, S.W., Myrdal, P.B., 2004. A theoretical and experimental analysis of formulation and device parameters affecting solution MDI size distributions. J. Pharm. Sci. 93, 2158–2175.
Steytler, D.C., Thorpe, M., Eastoe, J., Dupont, A., Heenan, R.K., 2003. Microemulsion formation in 1,1,1,2-tetrafluoroethane (R134a). Langmuir 19, 8715–8720.
Sun, Y., Shekunov, B.Y., 2003. Surface tension of ethanol in supercritical CO_2. J. Supercrit. Fluid 27, 73–83.
Svensson, B., Olsson, U., Alexandridis, P., Mortensen, K., 1999. A SANS investigation of reverse (water-in-oil) micelles of amphiphilic block copolymers. Macromolecule 32, 6725–6733.
Takishima, S., O'Neil, M.L., Johnston, K.P., 1997. Solubility of block copolymer surfactants in compressed CO_2 using a lattice fluid hydrogen-bonding model. Ind. Eng. Chem. Res. 36, 2821–2833.
Traini, D., Rogueda, P., Young, P., Price, R., 2005. Surface energy and interparticle force correlation in model pMDI formulations. Pharm. Res. 22, 816–825.
Traini, D., Young, P., Rogueda, P., Price, R., 2006. The use of AFM and surface energy measurements to investigate drug-canister material interactions in a model pressurized metered dose inhaler formulation. Aerosol Sci. Technol. 40, 227–236.
Tsujino, I., Yamazaki, T., Masutani, M., Sawada, U., Horie, T., 1999. Effect of Tween-80 on cell killing by etoposide in human lung adenocarcinoma cells. Cancer Chemother. Pharmacol. 43, 29–34.
Vervaet, C., Byron, P.R., 1999. Drug–surfactant–propellant interactions in HFA-formulations. Int. J. Pharm. 186, 13–30.
Warisnoicharoen, W., Lansley, A.B., Lawrence, M.J., 2003. Toxicological evaluation of mixtures of nonionic surfactants, alone and in combination with oil. J. Pharm. Sci. 92, 859–868.
Williams III, R.O., Liu, J., 1999. Formulation of a protein with propellant HFA 134a for aerosol delivery. Eur. J. Pharm. Sci. 7, 137–144.
Williams III, R.O., Liu, J., 1998. Influence of formulation additives on the vapor pressure of hydrofluoroalkane propellants. Int. J. Pharm. 166, 99–103.
Wu, L., Al-Haydari, M., da Rocha, S.R.P., 2008. Novel propellant-driven inhalation formulations: engineering polar drug particles with surface-trapped hydrofluoroalkane-philes. Eur. J. Pharm. Sci. 33, 146–158.
Wu, L., Bharatwaj, B., Panyam, J., da Rocha, S.R.P., 2007a. Core–shell particles for the dispersion of small polar drugs and biomolecules in hydrofluoroalkane propellants. Pharm. Res. 25, 289–301.
Wu, L., Peguin, R.P.S., da Rocha, S.R.P., 2007b. Understanding solvation in hydrofluoroalkanes: ab initio calculations and chemical force microscopy. J. Phys. Chem. B 111, 8096–8104.